Journal of Bioenergetics and Biomembranes, Vol. 33, No. 4, 2001

The Succinate Dehydrogenase from the Thermohalophilic Bacterium *Rhodothermus marinus*: Redox–Bohr Effect on Heme b_L[1]

Andreia S. Fernandes,[2] Manuela M. Pereira,[2] and Miguel Teixeira[2,3]

Received December 21, 2000; revised February 5, 2001

The succinate dehydrogenase from the thermohalophilic bacterium *Rhodothermus marinus* is a member of the succinate:menaquinone oxidoreductases family. It is constituted by three subunits with apparent molecular masses of 70, 32, and 18 kDa. The optimum temperature for succinate dehydrogenase activity is 80°C, higher than the optimum growth temperature of *R. marinus*, 65°C. The enzyme shows a high affinity for both succinate ($K_m = 0.165$ mM) and fumarate ($K_m = 0.10$ mM). It contains the canonical iron–sulfur centers S1, S2, and S3, as well as two B-type hemes. In contrast to other succinate dehydrogenases, the S3 center has an unusually high reduction potential of +130 mV and is present in two different conformations, one of which presents an unusual EPR signal with *g* values at 2.035, 2.009, and 2.001. The apparent midpoint reduction potentials of the hemes, +75 and −65 mV at pH 7.5, are also higher than those reported for other enzymes. The heme with the lower potential (heme b_L) presents a considerable dependence of the reduction potential with pH (redox–Bohr effect), having a $pK_a^{OX} = 6.5$ and a $pK_a^{red} = 8.7$. This behavior is consistent with the proposal that in these enzymes menaquinone reduction occurs close to heme b_L, near to the periplasmic side of the membrane, and involving dissipation of the proton transmembrane gradient.

KEY WORDS: Succinate dehydrogenase; *Rhodothermus marinus*; redox-Bohr.

INTRODUCTION

Succinate:quinone oxidoreductase (EC 1.3.5.1), or succinate dehydrogenase (SDH) is complex II in aerobic respiratory chains. It catalyzes the oxidation of succinate to fumarate, with the reduction of quinone, being also a component of the citric acid cycle. The enzyme is able to catalyze the reverse reaction, i.e., the reduction of fumarate to succinate, which occurs in anaerobic metabolism where fumarate is the last electron acceptor (Hägerhäll, 1997; Hederstedt and Ohnishi, 1992).

The structure of complex II was recently elucidated by X-ray crystallography (Iverson *et al.*, 1999; Lancaster *et al.*, 1999). It consists of a hydrophilic peripheral domain, facing the negative side of the membrane (bacterial periplasm) and a hydrophobic part that spans the membrane. The peripheral domain is composed by two subunits, one having a covalently bound FAD and another containing three different iron–sulfur clusters: $[2Fe–2S]^{2+/1+}$ (cluster S1), $[4Fe–4S]^{2+/1+}$ (cluster S2), and $[3Fe–4S]^{1+/0}$ (cluster S3). The hydrophobic domain is required for quinone reduction and functions as an anchor of the peripheral domain to the membrane. This domain, in the mitochondrial enzyme, has a B-Type heme as a prosthetic group, with a reduction potential of −185 mV (Hägerhäll, 1997; Hederstedt and Ohnishi, 1992).

The bacterial and archaeal enzymes are similar to the mitochondrial one, in contrast to the other complexes of the electron transfer chain, which in mitochondria present a larger number of subunits. Nevertheless, the enzymes

[1] Key to abbreviations: HiPIP, high-potential iron–sulfur protein; DCPIP, 2,6-dichlorophenolindophenol; DM, dodecyl β-D-maltoside; FRD, fumarate reductase; PMS, phenazine methosulfate; PMSF, phenylmethylsulfonyl fluoride; SDH, succinate dehydrogenase; TPTZ, 2,4,6-tripyridyl-*s*-triazine.

[2] Instituto de Tecnologia Química e Biológica, Universidade Nova de Lisboa, APT 127, 2780-156 Oeiras, Portugal.

[3] To whom all correspondence should be addressed. e-mail: miguel@itqb.unl.pt

0145-479X/01/0800-0343$19.50/0

from prokaryotes present some differences concerning the prosthetic groups and the anchor domain. In some archaeal enzymes, the $[3Fe–4S]^{1+/0}$ cluster is substituted by a second $[4Fe–4S]^{2+/1+}$ center (Janssen *et al.*, 1997; Gomes *et al.*, 1999). This modification was confirmed by amino acid sequence analyses of the iron–sulfur subunit that show the presence of an extra cysteine residue, providing a typical binding site for a $[4Fe–4S]^{2+/1+}$ cluster (Janssen *et al.*, 1997; Gomes *et al.*, 1999). The physiological relevance of this special feature has yet to be established. The anchoring domain is, in general, formed by one or two subunits containing one, two, or no B-type hemes. Again, in those archaeal enzymes, this domain is completely different: no hydrophobic subunits are present and the attachment must occur through an as yet unknown process [possibly by amphipatic helices present in subunit *c* (Lemos *et al.*, 2001)].

In SDHs containing two hemes—one has a low reduction potential (named heme b_L) and the other has a higher reduction potential (heme b_H). These hemes were tentatively assigned to the structure: heme b_L corresponds to the heme closer to the periplasm (also called distal heme, or b_D) and heme b_H to the one closer to the iron–sulfur subunit (proximal heme, or b_P) (Hägerhäll *et al.*, 1995).

The thermophilic bacterium *Rhodothermus marinus* has an unusual membrane-bound respiratory chain (Pereira *et al.*, 1994, 1999a,b,c, 2000a), containing a new complex III (a cytochrome *bc* complex; Pereira *et al.*, 1999a), and a HiPIP (Pereira *et al.*, 1994, 1999b) as an electron carrier between this complex and the caa_3 oxidase, which has a different proton pathway (Pereira *et al.*, 1999c, 2000b). The presence of its dehydrogenases was investigated in intact membranes by EPR spectroscopy (Pereira *et al.*, 1999b). It was shown that its succinate dehydrogenase has a $[3Fe–4S]^{1+/0}$ center with an unusually high reduction potential of +130 mV and having two conformations, one of which presents an unusual EPR signal. To further investigate both the origin of this heterogeneity and elucidate the *R. marinus* respiratory chain, its succinate dehydrogenase was purified and characterized, addressing simultaneously the redox properties in a succinate dehydrogenase using a low-potential electron acceptor—menaquinone.

MATERIALS AND METHODS

Protein Purification

Bacterial growth, membrane preparation, and solubilization were done as described in Pereira *et al.* (1999a). All chromatographic steps were done on Pharmacia HiLoad or LKB-HPLC systems, at 4°C. The detergent-solubilized membrane fraction was applied to a fast-flow DEAE column, using as buffer 20 mM Tris–HCl pH 8, 0.1% DM and eluted in a linear gradient of 0 to 50% 1 M NaCl. The SDH-containing fraction was then applied to a chelating sepharose fast-flow column saturated with Ni^{2+} and equilibrated with 20 mM Tris–HCl pH 8, 0.1% DM. The fraction containing the SDH was eluted when washing the column with buffer before the imidazole gradient, being then applied to a Q-sepharose column. This column was eluted in 20 mM Tris–HCl pH 8, 0.1% DM with a linear gradient of 0 to 50% 1 M NaCl. The enzyme was then applied to a HTP column, eluted with a linear gradient of 0 to 500 mM potassium phosphate, and then to a gel filtration S200 column, eluted with 20 mM Tris–HCl pH 8, 0.1% DM, 200 mM NaCl. The fraction containing the SDH complex was finally purified in a Mono Q column, and eluted in 20 mM Tris–HCl pH 8, 0.1% DM. Two linear gradients of 0 to 22% and 22 to 50% NaCl were applied, the SDH having eluted in the second gradient. All buffers included 1 mM PMSF and 1 mM EDTA, with the exception of the chelating sepharose column. After all purification steps, the visible and EPR spectra were monitored and activity assays were performed.

Protein, Heme and Iron Determination

Protein concentrations were determined using the modified microbiuret method for membrane proteins (Watters, 1978). Nonheme iron concentration was determined using the TPTZ method (Fisher and Price, 1964). The heme content was determined from redox spectra using a molar absorbivity of $\varepsilon = 22 \times 10^3\ M^{-1}/cm$ at the α-band maximum per heme (Wood, 1984).

Heme Extraction and HPLC Analysis

Noncovalently bound hemes were extracted according to Lübben and Morand (1994). Heme composition was analyzed on a System Gold, Beckman chromatograph with a Deltapak C18 (3.9 × 150 mm, Waters) reverse-phase HPLC column. Hemin from Sigma was used as a standard.

Electrophoresis

Molecular masses were determined by 15–20% linear gradient SDS–PAGE performed in a Laemmli discontinuous buffer system. The sample buffer contained 8 M urea and 10% SDS to ensure an efficient exchange

of detergent and denaturation. The gel was stained with Coomassie blue.

Amino Acid Sequencing

For peptide sequencing, the enzyme subunits were separated by the electrophoresis procedure described above and transferred to a polyvinylidene difluoride (PVDF) membrane. Each transblotted sample was submitted to N-terminal protein sequence analysis by automated Edman degradation (Edman and Begg, 1967), using an Applied Biosystem model 470A sequencer.

Spectroscopic Techniques

Electronic spectra were obtained on a Beckman DU-70 or on an OLIS DW2 spectrophotometers, at room temperature. EPR spectra were obtained as in Pereira *et al.* (1999a). The samples were dissolved in 20 mM Tris–HCl pH 7.5, 0.1% DM buffer.

Catalytic Activity Assays

Succinate: DCPIP oxidoreductase activity was monitored by following the PMS-coupled reduction of DCPIP at 578 nm ($\varepsilon = 18 \times 10^3$ M^{-1}/cm). The reaction mixture contained 80 mM potassium phosphate pH 7.5, 0.1% DM buffer, 0.05 mM PMS, and 0.05 mM DCPIP. The reaction was started by the addition of SDH. Benzyl viologen:fumarate oxidoreductase activity was monitored anaerobically by following the oxidation of benzyl viologen at 578 nm ($\varepsilon = 7.8 \times 10^3$ M^{-1}/cm). The reaction mixture contained 100 mM potassium phosphate pH 6.5, 0.1% DM buffer, 0.3 mM benzyl viologen reduced with dithionite and sample. The reaction was started by the addition of fumarate.

Redox Titrations

Anaerobic potentiometric titrations were followed by visible spectroscopy, at room temperature and at different pH values, from 5.5 to 9, with the following as redox mediators (each at a final concentration of 2 μM): 1,2-naphtoquinone, phenazine methosulfate, 1,4-naphtoquinone, methylene blue, tetramethyl-*p*-benzoquinone, menadione, plumbagin, phenazine, 2-hydroxyl-1,4-naphtoquinone. A combined silver/silver chloride electrode was used, calibrated with a saturated quinhydrone solution. Spectra were measured from 400 to 700 nm, and analyzed by manual deconvolution using the Matlab software, as described in Pereira *et al.* (1999a). The redox potentials are quoted in relation to the standard hydrogen electrode.

RESULTS AND DISCUSSION

Isolation and Biochemical Characterization

The succinate dehydrogenase from *R. marinus* was purified to homogeneity and three bands observed in a SDS–PAGE, with apparent molecular masses of 70, 32, and 18 kDa (data not shown), which are in agreement with the molecular masses reported for other succinate dehydrogenases (Table I). The N-terminal sequences for these subunits allow the clear identification of the 70 kDa protein as the flavosubunit and the 32 kDa one as the iron–sulfur subunit (Fig. 1), as both exhibit considerable identities or similarities with homologous proteins: 30–58% identity and 47–75% similarity for the flavosubunit; 23–46% identity and 50–69% similarity for the iron–sulfur subunit.

Table I. Subunit Composition of Some Succinate Dehydrogenases[a]

Organism	Molecular masses (kDa)				Reference
	Flavin subunit	Iron–sulfur subunit	Anchor Subunit		
Rhodothermus marinus	70	32	18	—	This work
Escherichia coli	71	26	17	15	Condon *et al.*, 1985
Neurospora crassa	72	28	14	—	Weiss and Headon, 1979
Bos taurus	74	26	15.8	14.9	Tushurashvili *et al.*, 1985
Paracoccus denitrificans	64.9	28.9	13.4	12.5	Pennoyer *et al.*, 1988
Desulfobulbus elongatus	68.5	27.5	22	—	Samain *et al.*, 1987
Bacillus firmus OF4	64.5	28.5	16	—	Gilmour and Krulwich, 1996
Bacillus subtilis	65	28	23	—	Hägerhäll *et al.*, 1992
Sulfolobus acidocaldarius	66	31	28	12.8	Moll and Schäfer, 1991

[a] Sub., subunit.

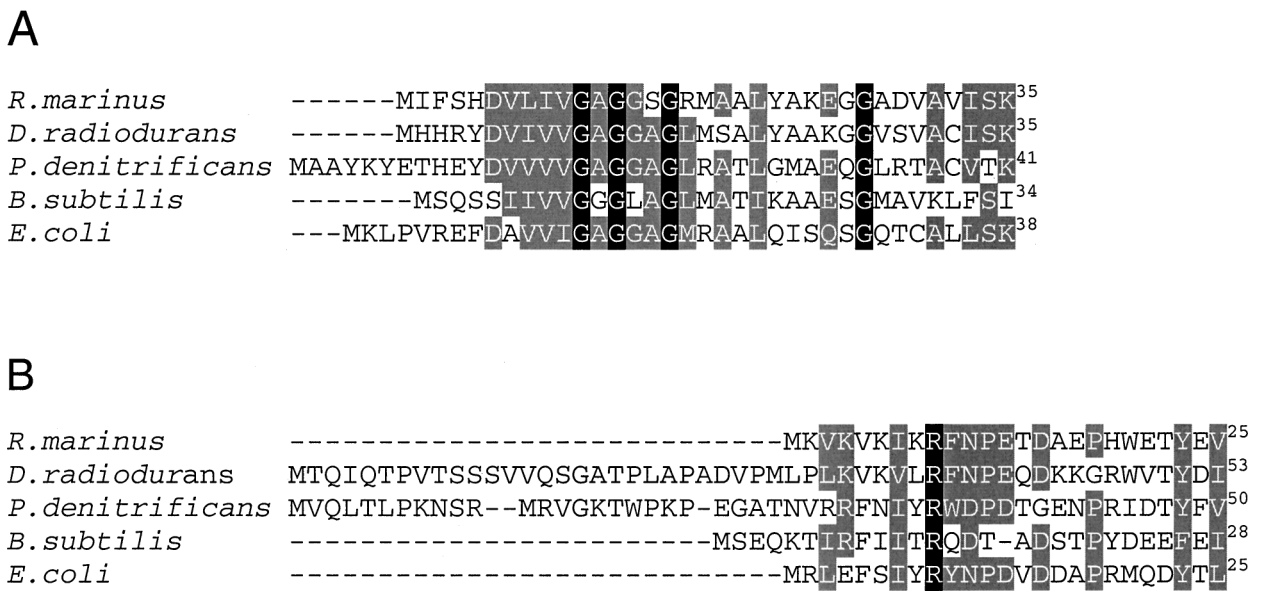

Fig. 1. N-terminal amino acid sequence alignment of SDH flavoprotein (A) and iron-sulfur protein (B). *R.*, *Rhodothermus*, *D.*, *Deinococcus* [acc. no. 7473936 (A) and 7473937 (B)], *P.*, *Paracoccus* [acc. no. 1125261 (A) and 11252609 (B)], *B.*, *Bacillus* [acc. no. 1071812 (A) and 1075923 (B)], *E.*, *Escherichia* [acc. no. 1786942 (A) and 1786943 (B)]. Strictly conserved amino acid residues are shaded in black and almost strictly conserved and strongly similar residues are shaded in grey.

The N-terminal sequence of the lowest molecular mass subunit does not show similarities with other known sequences (data not shown), which is not surprising since this subunit is most probably the anchoring domain and this type of proteins are very divergent.

The pyridine hemochrome spectrum shows an α-peak with a maximum at 553.5 nm (not shown), which is slightly lower than those reported for B-type hemes. However, heme extraction and HPLC analysis established that *R. marinus* succinate-dehydrogenase contains only B-type hemes. The ratio of heme:nonheme iron (determined by the TPTZ method) concentrations determined was 2:9, which correlates with the presence of two hemes and nine iron atoms from the three iron–sulfur centers per molecule.

The purified succinate dehydrogenase presents a turnover number of 79.6 s^{-1}, at 65°C, approximately twice that of the *E. coli* enzyme, at 25°C (Kita *et al.*, 1989). However, the optimum temperature for the succinate dehydrogenase activity is 80°C (Fig. 2A), which is higher than the optimum temperature growth of *R. marinus* (65°C). From the Arrhenius plot (Fig. 2B), an apparent activation energy of 48.2 kJ/mol^{-1}/K^{-1} was calculated. The K_m for succinate was determined to be 0.165 mM, at 65°C (Fig. 2C), which is one of the lowest reported for these enzymes (Table II), indicating a high affinity for the substrate.

Table II. Comparison of K_m for Succinate of Several Succinate Dehydrogenases (SDH) and Fumarate Reductases (FRD)

Organism	Enzyme	K_m for succinate (mM)	Reference
Rhodothermus marinus	SDH	0.165	This work
Sulfolobus acidocaldarius	SDH	1.42	Moll and Schäfer, 1991
Halobacterium halobium	Membranes	0.7	Gradin *et al.*, 1985
Bacillus firmus OF4	SDH	0.30	Gilmour and Krulwich, 1996
Acidianus ambivalens	Membranes	0.50	Gomes *et al.*, 1999
Bos taurus	SDH	0.020	Tushurashvili *et al.*, 1985
Thermoplasma acidophilum	Membranes	0.32	Anemüller *et al.*, 1995
Sulfolobus strain 7	Membranes	0.28	Iwasaki *et al.*, 1995
Escherichia coli	SDH	0.071	Kita *et al.*, 1989
Escherichia coli	FRD	1.0	Ingledew and Poole, 1984
Wolinella succinogenes	FRD	7	Unden *et al.*, 1980

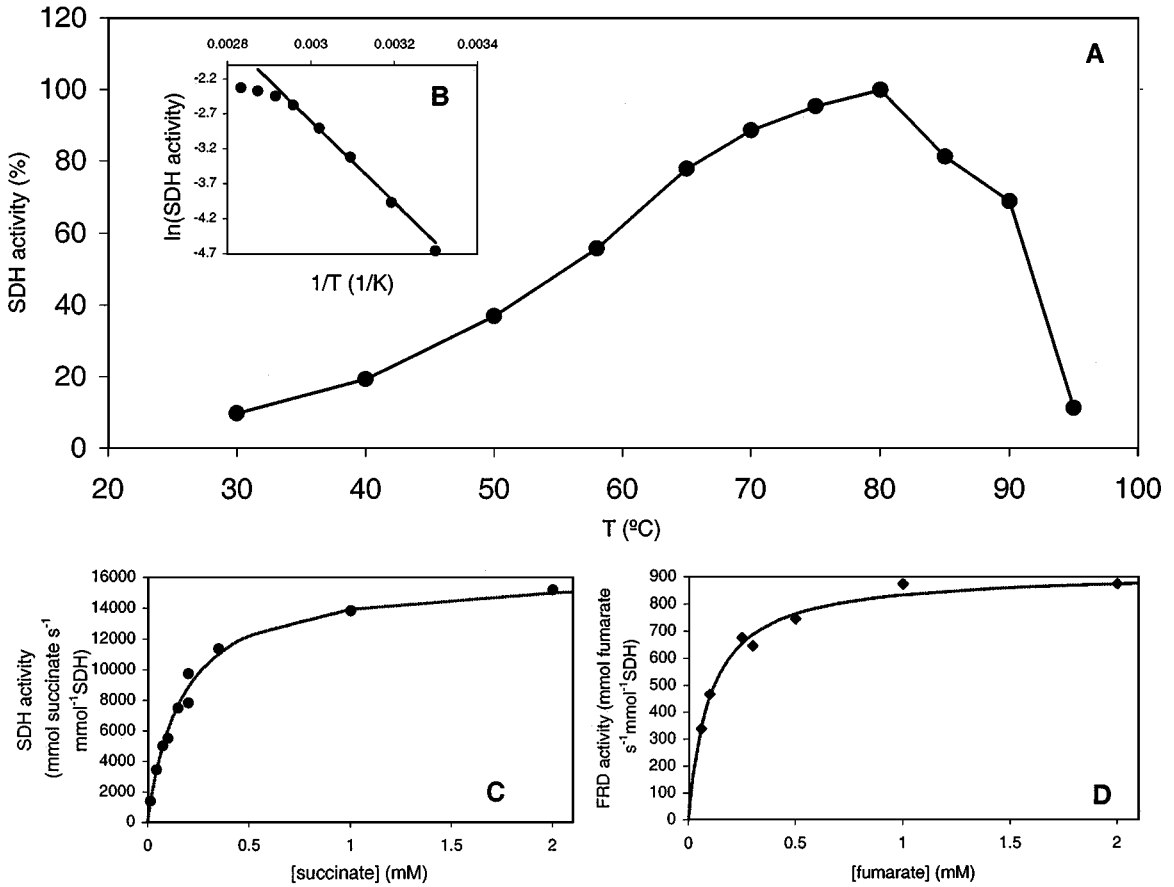

Fig. 2. (A) Temperature profile of SDH activity of *R. marinus* succinate dehydrogenase. (B) Arrhenius plot of the data from A. (C) Michaelis-Menten hyperbola of *R. marinus* SDH with succinate as substrate. (D) Michaelis-Menten hyperbola of *R. marinus* SDH with fumarate as substrate. In (C) and (D) the assays were performed at 65°C. The solid curves were calculated with the parameters presented in the text.

The enzyme is also able to catalyze the reverse reaction, reduction of fumarate, with a K_m 0.10 mM at 65°C (Fig. 2D).

Spectroscopic Characterization

The electronic absorption spectra of *R. marinus* SDH in the oxidized and reduced states are typical of heme proteins (Fig. 3), containing iron–sulfur and flavin as other prosthetic groups (yielding a broad absorption from ~380 to 450 nm, underneath the heme Soret band, still discernable as a broad feature at ca. 450 nm).

The spectrum of the dithionite-reduced minus oxidized *R. marinus* succinate dehydrogenase has a Soret band with a maximum at 425 nm and presents an α-band with a maximum at 557 nm (Fig. 3B,b). This spectrum could be deconvoluted by successive reductions with different reducers (Fig. 3B). Thus, upon reduction with succinate or ascorbate (Fig. 3B,a) a very broad band in the α region with a maximum at 559 nm is observed corresponding to the reduction of the heme with the higher reduction potential (see below). The spectrum of the second heme could be obtained by reduction with dithionite and subtraction of the previous spectrum. In this case, the α band is much narrower presenting a maximum at 556 nm. Integration of the areas of both α bands shows that the hemes are present in the same proportion.

In the oxidized form, the purified enzyme shows an unusual EPR spectrum with g values at 2.035, 2.009, and 2.001 and 2.025, 2.002, and 2.000, attributed to two different conformations of the oxidized $[3Fe–4S]^{1+/0}$ center (S2) (Fig. 4A) (Pereira *et al.*, 1999b). This type of signal has been reported previously as a result of damaged $[4Fe–4S]^{2+/1+}$ centers; however, in *R. marinus* SDH, this

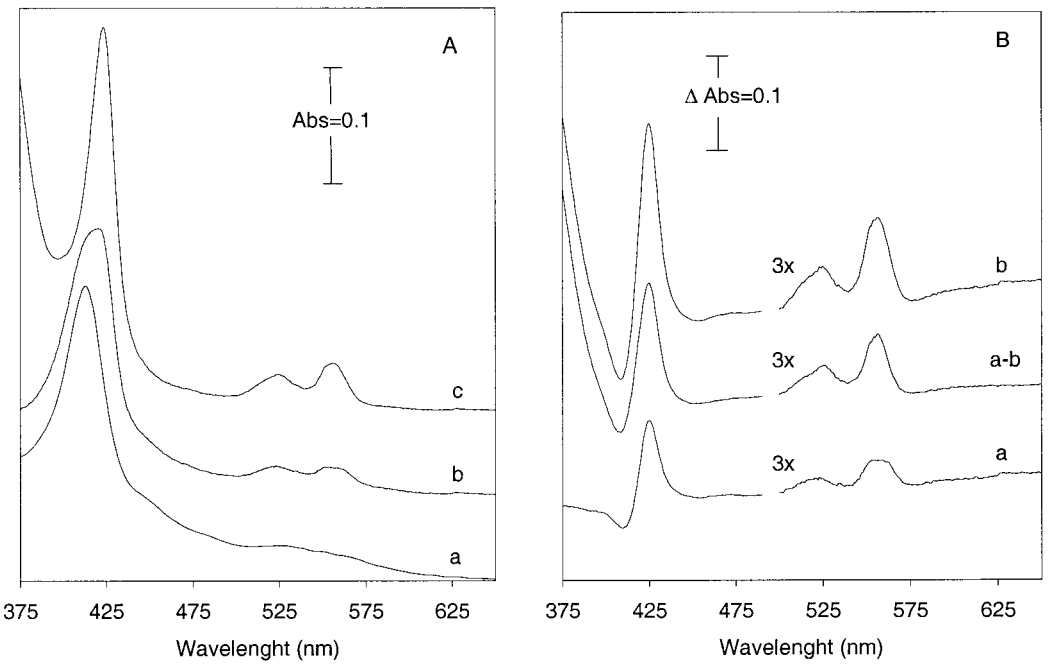

Fig. 3. (A) Visible spectra of *R. marinus* SDH in the oxidized state (a), and upon reduction with succinate (b) and ditionite (c). (B) Difference visible spectra of *R. marinus* succinate dehydrogenase: a, reduction with sodium succinate, b, total reduction with sodium dithionite.

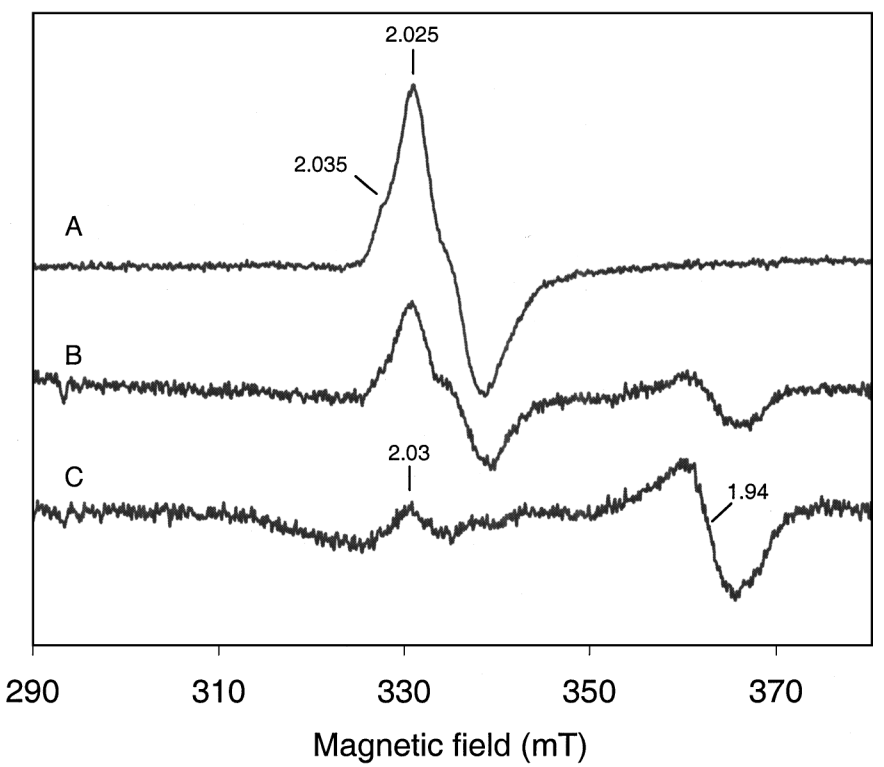

Fig. 4. EPR spectra of *R. marinus* SDH. (A) As isolated (oxidized form); (B) upon addition of succinate; and (C) upon addition of dithionite. Temperature: 10 K; microwave frequency; 9.64 GHz; microwave power: 2.4 mW; modulation amplitude: 0.9 mT.

feature was observed also in intact cells and membranes (Pereira *et al.*, 1999b), which shows that it is not due to any degradation occurring during purification. This is further supported by its low K_m and high turnover number, which indicate that it is highly active as purified. Therefore, the observed heterogeneity is not related to an inactive form of the enzyme and, at present, its origin remains unknown. Incubation of *R. marinus* SDH with sodium succinate (∼30 mM) leads to the bleaching of the EPR resonances at $g \sim 2$ and development of a quasiaxial signal with g values of 2.030 and 1.939 (Fig. 4B). Particularly well observed at 20 K and observable up to ∼70 K without noticeable broadening, this resonance is similar to that of the reduced binuclear $[2Fe–2S]^{2+/1+}$ (center S1) from *Escherichia coli* SDH (Morningstar *et al.*, 1985; Maguire *et al.*, 1985; Hederstedt and Ohnishi, 1992). It was found that together the $g = 2.035$ and 2.025 species quantitate for one center S1, in relation to the intensity of the resonance of center S2. This was observed by both manual double integration of the experimental spectra of these preparations obtained under nonsaturating conditions and using the respective theoretical simulations. Upon reduction with dithionite, only a slight increase in intensity of the S1 signal is observed (Fig. 4C). From the power dependence of the intensity of this signal, it could be inferred the presence of the reduced $[4Fe–4S]^{2+/1+}$ center (data not shown): the power of half-saturation of center S1 in the succinate-reduced enzyme (0.3 mW) increases to 1.7 mW upon reduction with dithionite, which means that there is a faster spin relaxation of center S1 when the sample is totally reduced. This suggests the interaction of center S1 with other center, cluster S3 (e.g., Anemüller *et al.*, 1995).

Redox Behavior Monitored by Visible Spectroscopy

The reduction potential of the $[3Fe–4S]^{1+/0}$ center was previously determined by EPR-monitored redox titration to be +130 mV (Pereira *et al.*, 1999b), which is much higher than what was reported for other SDHs (Hägerhäll, 1997).

The redox titrations of the hemes of *R. marinus* succinate dehydrogenase were carried out at different pH values from 5.5 to 9 (Fig. 5). In every case, two redox transitions were observed. Since the two hemes have distinct visible spectra in the α-region, each transition can be, at least in part, assigned to a different heme. Both transitions present a redox–Bohr effect, i.e., the reduction potentials are pH dependent. At pH 7.5, the transitions occur at midpoint

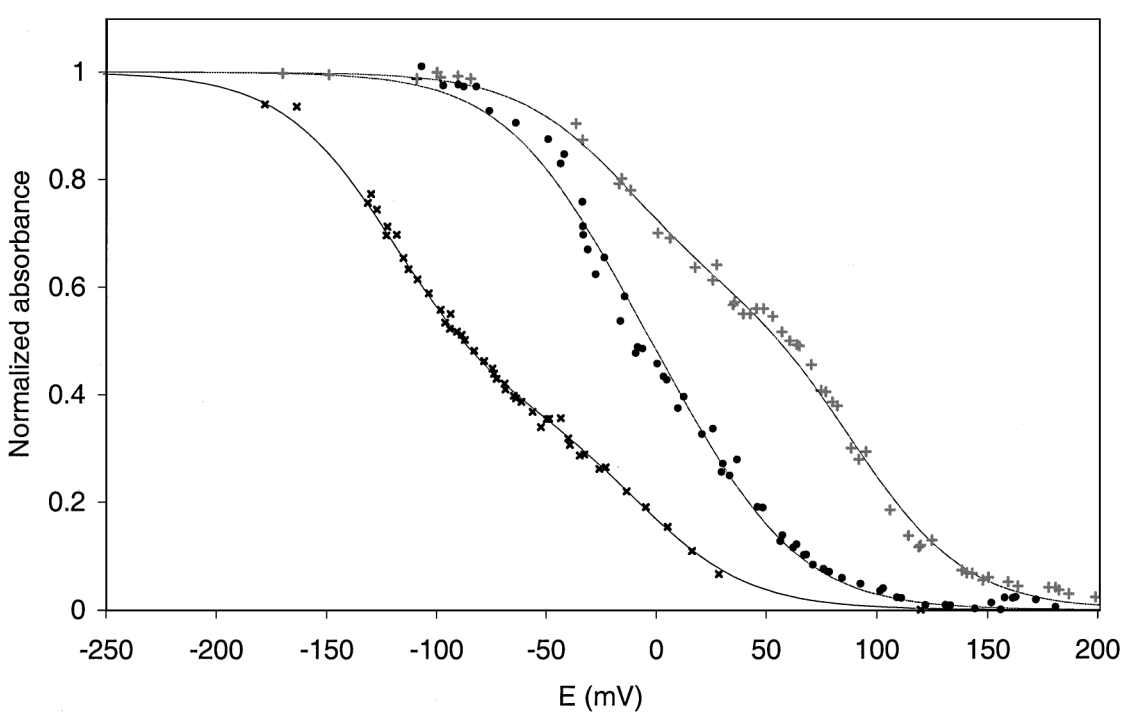

Fig. 5. Redox titrations of *R. marinus* SDH hemes at pH 5.5 (+), 6.5 (•) and 8.5 (×). The lines were calculated with Nernst equations for two independent processes with the following midpoint reduction potentials: +90 mV, −10 mV (pH 5.5); +25 mV, −30 mV (pH 6.5), and −7 mV, −120 mV (pH 8.5).

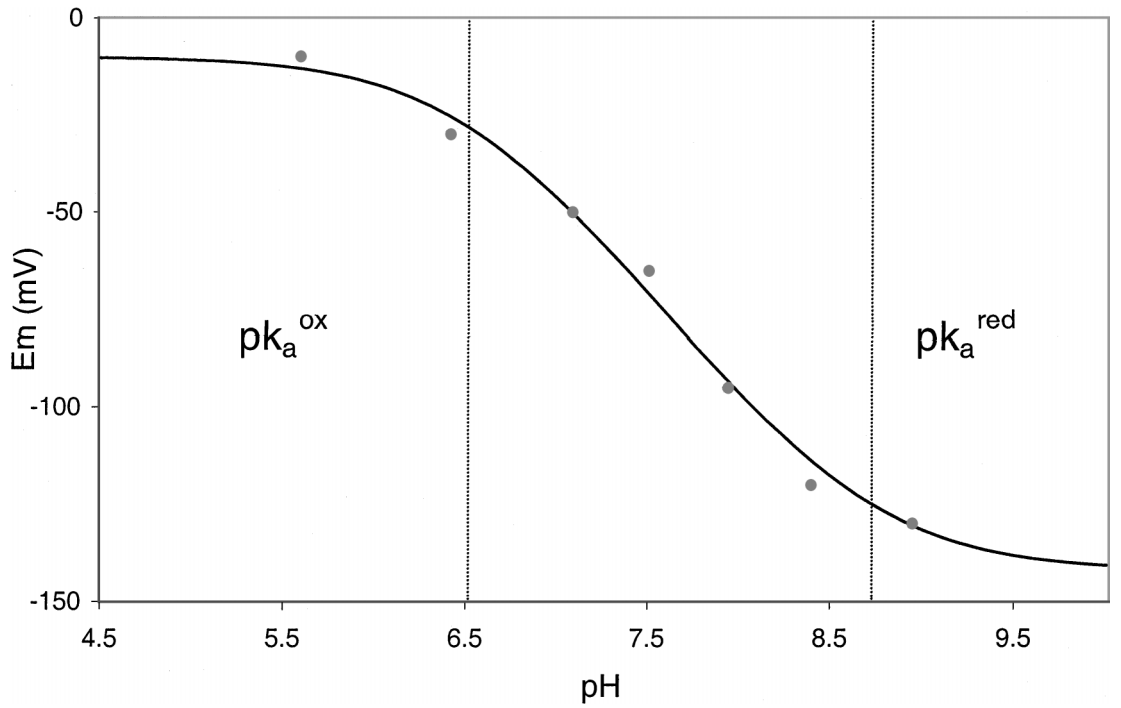

Fig. 6. pH dependence of the midpoint reduction potential of the heme b_L of *R. marinus* SDH. The solid line was calculated for a single ionization, with $pK_a^{ox} = 6.5$ and $pK_a^{red} = 8.7$, using the following equation:

$$E = E_A + \frac{RT}{F}\ln\left(\frac{K_{Red} + [H^+]}{K_{Ox} + [H^+]}\right)$$

where E_A is the apparent reduction potential for the acid form.

potentials of +75 and −65 mV. While the high potential transition in other SDHs occurs generally from ∼−20 to +75 mV, as for the *R. marinus* enzyme, the low potential one occurs below ∼−150 (Hägerhäll, 1997; Lancaster *et al.*, 2000), a value much lower than that of *R. marinus* SDH. For the low-potential transition (Fig. 6), the pH dependence can be described by the effect of a single proton ionization, with pK_a^{ox} and pK_a^{red} values of 6.5 and 8.7, respectively. For the high-potential heme, the pH dependence is less clear and the data obtained did not allow the determination of the pK_a values associated with it (data not shown). The structure of *Wollinella succinogens* fumarate reductase (Lancaster *et al.*, 1999) shows that the heme b_L propionates are not hydrogen bonded to protonatable residues. Thus, the redox–Bohr effect may be due to the ionization of the heme propionates or, upon reduction, to a change of the hydrogen bond network, eventually leading to the solvent. It should be noted that in that enzyme the quinone binds close to heme b_L and interacts with a glutamate (Glu66), a putative acceptor of the proton released by the quinone oxidation (Lancaster *et al.*, 2000).

The succinate dehydrogenases are an example of redox proteins where a unique determination of the intrinsic reduction potentials is not possible. In fact, the crystal structure of the fumarate reductase from *Wolinella succinogens* (Lancaster *et al.*, 1999) shows that the hemes are quite close to each other (the minimum distance is ca 4.1 Å). Thus, on pure electrostatic terms, a strong anticooperativity in their reduction is expected, due to electrostatic repulsion. The same occurs most probably in the iron–sulfur subunit, as the distances between each cluster are small, ca. 10 Å. This anticoperative redox behavior can be partially or even totally overcomed by redox-dependent structural changes and/or coupling with proton ionization equilibria. Since the microstates formed on-going from the fully oxidized to the fully reduced states (considering just the heme subunit, four microstates) can not be spectrally identified, it is not possible to uniquely determine the intrinsic potentials of the metal centers. In fact, the titration curves can be equally described either by just the sum of two Nernst equations for two independent redox processes or by an interactive system of two redox centers with a variable interaction potential. Nevertheless, the possibility of both hemes having the same reduction potential can be ruled out in this enzyme, as the hemes have distinct absorption characteristics, but

the potentials obtained represent only the apparent midpoint potentials of the redox transitions of the whole enzyme.

The mechanism of operation of succinate:menaquinone oxidoreductases is still intriguing since it oxidizes succinate with a higher reduction potential ($E^0 = +30$ mV) than menaquinone, which is reduced to menaquinol with a reduction potential of -74 mV, being thus a thermodynamically unfavorable reaction. Several steps of intramolecular electron transfer are also thermodynamically unfavorable. One of such cases is the uphill electron transfer from the high- to the low-potential heme, although it should be recalled again that strong electrostatic interactions are expected to occur among all the redox centers of these enzymes. It was proposed that this problem may be overcomed by the membrane potential (Schirawski and Unden, 1998), which could be used to make that transfer possible. It also appears that in the case of these succinate dehydrogenases, the quinone binding site is located close to the periplasm (Lancaster *et al.*, 2000) and thus the uptake of protons for the quinone reduction comes from this side, contributing to a dissipation of the transmembrane proton gradient. The observation that in the *R. marinus* enzyme the low-potential heme, presumably situated closer to the periplasm, has a redox–Bohr effect, suggests that this heme may be intervening in proton uptake and direct reduction of the quinone, by electron transfer and proton uptake. Thus it can be hypothesized that upon reduction of the low-potential heme, one proton is uptaken from the periplasm and upon reoxidation by the quinone the pK_a of the heme changes and the same proton leaves the heme region and is transfered to the quinone.

In the case of the high-potential heme, the pH dependence of its potential may result from the electrostatic interaction with the other heme, i.e., if the reduction potential of one heme changes, the reduction potential of the other has also to change.

In conclusion, the succinate dehydrogenase from *R. marinus*, in spite of its peculiar spectroscopic properties, is a canonical member of the succinate:menaquinone oxidoreductase family. It was further shown that the hemes of *R. marinus* enzyme have a pH-dependent reduction potential, with a pK_a in a physiological range, which may be an important behavior for the functioning of such enzymes.

ACKNOWLEDGMENTS

A. S. Fernandes and M. M. Pereira are recipients of grants from Praxis XXI program (BD/1163/00 and BPD/22054/99). The work was supported by FCT Project 36560/99.

J.-J. Bourgois thanks Dr. T. Seppi and Dr. G. Stubauer, Universitätsklinik für Strahlentherapie und Radioonkologie, Universität Innsbruck, Anichstrasse 35, A-6020 Innsbruck, Austria for giving access to the "Oxytron" facility and providing the relevant theoretical and technical assistance.

The work in Austria was supported by travel funds from the Laboratoire dePhysiologie Animale, Université Catholique de Louvain, Louvain-La-Neuve, Belgium.

J.-J. Bourgois also thanks Mr. D. Jeuniaux, Center for Oxygen Research and Development, Institut de Chimie, B6a, Domaine du Sart Tilman, Université de Liège, B-4000 Liège, Belgium for his generous technical support in data acquisition systems.

REFERENCES

Anemüller, S., Hettmann, T., Moll, R., Teixeira, M., and Schäfer, G. (1995). *Eur. J. Biochem.* **232**, 563–568.
Condon, C., Cammack, R., Patil, D. S., and Owen, P. (1985). *J. Biol. Chem.* **260**, 9427–9434.
Edman, P. and Begg, G. (1967). *Eur. J. Biochem.* **1**, 80–90.
Fisher, D. S. and Price, D. C. (1964). *Clin. Chem.* **10**, 21–31.
Gilmour, S. and Krulwich, T. A. (1996). *Biochim. Biophys. Acta* **1276**, 57–63.
Gomes, C. M., Lemos, R. S., Teixeira, M., Kletzin, A., Huber, H., Stetter, K. O., Schäfer, G., and Anemüller, S. (1999). *Biochim. Biophys. Acta* **1411**, 134–141.
Gradin, C. H., Hederstedt, L., and Baltscheffsky, H. (1985). *Arch. Biochem. Biophys.* **239**, 200–205.
Hägerhäll, C. (1997). *Biochim. Biophys. Acta* **1320**, 107–141.
Hägerhäll, C., Aasa, R., von Wachenfeldt, C., and Hederstedt, L. (1992). *Biochemistry* **31**, 7411–7421.
Hägerhäll, C., Fridén, H., Aasa, R., and Hederstedt, L. (1995). *Biochemistry* **34**, 11080–11089.
Hederstedt, L. and Ohnishi, T. (1992). In *Molecular Mechanisms in Bioenergetics*, Chap. 7, L. Ernster, Ed., Elsevier, Amsterdam, pp. 163–198.
Ingledew, W. J. and Poole, R. K. (1984). *Microbiol. Rev.* **48**, 222–271.
Iverson, T. M., Luna-Chavez, C., Cecchini, G., and Rees, D. C. (1999). *Science* **284**, 1961–1966.
Iwasaki, T., Wakagi, T., and Oshima, T. (1995). *J. Biol. Chem.* **270**, 30902–30908.
Janssen, S., Schäfer, G., Anemuller, S., and Moll, R. (1997). *J. Bacteriol.* **179**, 5560–5569.
Kita, K., Vibat, C. R. T., Meinhardt, S., Guest, J. R., and Gennis, R. B. (1989). *J. Biol. Chem.* **264**, 2672–2677.
Lancaster, C. R. D., Kroger, A., Auer, M., and Michel, H. (1999). *Nature* (*London*) **402**, 377–385.
Lancaster, C. R. D., Groß, R., Hass, A., Mäntele, W., Simon, J., and Kröger, A. (2000). *Proc. Nat. Acad. Sci. USA* **97**, 13051–13056.
Lemos, R. S., Gomes, C. M., and Teixeira, M. (2001). *Biochem. Biophys. Res. Commun.* **281**, 141–150.
Lübben, M. and Morand, K. (1994). *J. Biol. Chem.* **269**, 21473–21479.
Maguire, J., Johnson, M. K., Morningstar, J. E., Ackrell, B. A. C., and Kearney, E. B. (1985). *J. Biol. Chem.* **260**, 10909–10912.
Moll, R. and Schäfer, G. (1991). *Eur. J. Biochem.* **201**, 593–600.

Morningstar, J. E., Johnson, M. K., Cecchini, G., Ackrell, B. A. C., and Kearney, E. B. (1985). *J. Biol. Chem.* **260**, 13631–13638.
Pennoyer, J. D., Ohnishi, T., and Trumpower, B. L. (1988). *Biochim. Biophys. Acta* **935**, 195–207.
Pereira, M. M., Antunes, A. M., Nunes, O. C., Costa, M. S., and Teixeira, M. (1994). *FEBS Lett.* **352**, 327–330.
Pereira, M. M., Carita, J. N., and Teixeira, M. (1999a). *Biochemistry* **38**, 1268–1275.
Pereira, M. M., Carita, J. N., and Teixeira, M. (1999b). *Biochemistry* **38**, 1276–1286.
Pereira, M. M., Santana, M., Soares, C. M., Mendes, J., Carita, J. N., Fernandes, A. S., Saraste, M., Carrondo, M. A., and Teixeira, M. (1999c). *Biochim. Biophys. Acta* **1413**, 1–13.
Pereira, M. M., Carita, J. N., Anglin, R., Saraste, M., and Teixeira, M. (2000a). *J. Bioenerg. Biomembr.* **32**, 143–152.
Pereira, M. M., Verkhovskaya, M. L., Teixeira, M., and Verkhovsky, M. I. (2000b). *Biochemistry* **39**, 6336–6340.
Samain, E., Patil, D. S., DerVartanian, D. V., Albagnac, G., and LeGall, J. (1987). *FEBS Lett.* **216**, 140–144.
Schirawski, J. and Unden, G. (1998). *Eur. J. Biochem.* **257**, 210–215.
Tushurashvili, P. R., Gavrikova, E. V., Ledenev, A. N., and Vinigradov, A. D. (1985). *Biochim. Biophys. Acta* **809**, 145–159.
Unden, G., Hackenberg, H., and Kröger, A. (1980). *Biochim. Biophys. Acta* **591**, 275–288.
Watters, C. (1978). *Anal. Biochem.* **88**, 695–698.
Weiss, G. and Headon, D. R. (1994). *Eur. J. Biochem.* **99**, 139–149.
Wood, P. M. (1984). *Biochim. Biophys. Acta* **768**, 293–317.